

MILLIMETER WAVE COMMUNICATIONS: FROM POINT-TO-POINT LINKS TO AGILE NETWORK CONNECTIONS

A Project Report

submitted by

SANCHIT GUPTA

in partial fulfilment of requirements

for the award of the dual degree of

BACHELOR OF TECHNOLOGY AND MASTER OF TECHNOLOGY



**DEPARTMENT OF ELECTRICAL ENGINEERING
INDIAN INSTITUTE OF TECHNOLOGY MADRAS**

MAY 2018

THESIS CERTIFICATE

This is to certify that the thesis titled "**MILLIMETER WAVE COMMUNICATIONS: FROM POINT-TO-POINT LINKS TO AGILE NETWORK CONNECTIONS**", submitted by **Sanchit Gupta**, to the Indian Institute of Technology Madras, for the award of the dual degree of **Bachelor of Technology and Master of Technology** in Electrical Engineering, is a bona fide record of the research work done by him under my supervision. The contents of this thesis, in full or in parts, have not been submitted to any other Institute or University for the award of any degree or diploma.



Dr. Srikrishna Bhashyam
Project Advisor
Professor
Dept. of Electrical Engineering
IIT Madras, 600036

Place: Chennai

Date: 9th May 2018

ACKNOWLEDGEMENTS

I express my sincere gratitude to Prof. Srikrishna Bhashyam for advising me on my Dual Degree project. His valuable help and patience has helped me sail through the duration of the project.

I would also like to thank my lab-mate, Silpa Nair, without whose help it would have been very difficult to complete the project in time.

I would like to thank my parents and my sister for their consistent support and motivation. Talking to them has helped me a lot and fueled me everyday, encouraged me to keep working even when I was far away from home.

Finally, I would like to thank the department, the institute, the professors, my lab-mates, and my friends for their contribution during the tenure of my stay in the campus.

ABSTRACT

KEYWORDS: Millimeter Waves, Beam Steering, Agile-Link, MIMO, Hashing, Voting, Pencil Beams

The fifth generation (5G) of cellular communication will be based on millimeter waves, and thus will use massive MIMO systems and highly directional antennas to focus their power on the receiver using pencil beams. We discuss an algorithm, Agile-Link (Abari *et al.*, 2016), which is a mmWave beam steering algorithm that is demonstrated to find the correct beam alignment without scanning the whole space exhaustively, a process which takes upto a few seconds. The delay in the latter method is problematic in a situation, where the base station needs to quickly switch between users and accommodate huge number of mobile clients. Instead of scanning, the algorithm hashes the beam directions into bins using suitable hash functions. It then identifies the correct beam alignment by checking how the energy changes over the different hash functions. In this thesis, simulations are done to verify the working of this algorithm.

TABLE OF CONTENTS

| | |
|--|-----------|
| ACKNOWLEDGEMENTS | i |
| ABSTRACT | ii |
| LIST OF FIGURES | iv |
| ABBREVIATIONS | v |
| NOTATION | vi |
| 1 INTRODUCTION | 1 |
| 1.1 Motivation | 1 |
| 1.2 Beam Formation and Steering | 2 |
| 1.3 Thesis Outline | 2 |
| 2 SYSTEM | 3 |
| 3 Agile-Link Algorithm | 5 |
| 3.1 The Algorithm | 5 |
| 3.1.1 Hashing Spatial Directions into Bins | 5 |
| 3.1.2 Recovering the Directions of the Paths | 8 |
| 3.2 Illustrative Example | 9 |
| 3.3 Measurement Complexity | 10 |
| 4 LITERATURE SURVEY | 11 |
| 5 EXPERIMENTS | 12 |
| 6 SIMULATION RESULTS | 14 |
| 7 CONCLUSION | 21 |

LIST OF FIGURES

| | | |
|------|--|----|
| 1.1 | EM Spectrum showing vast availability of mmWaves. Source: Electronic Design 'What to Expect with 5G' | 1 |
| 2.1 | Omnidirectional Tx and Phased Array Rx Antenna | 3 |
| 2.2 | Phased Array Architecture; Source: Abari <i>et al.</i> (2016) | 4 |
| 3.1 | A wider beam to hash the space cannot be created since it requires changing the size of the array; Source: Abari <i>et al.</i> (2016) | 6 |
| 3.2 | 'Hashing well-spread functions into a bin. The beams in the first figure are 60° apart' and 'Bins in a hash function. The beams with the same colour are hashed into the same bin'; Source: Abari <i>et al.</i> (2016) | 7 |
| 3.3 | Illustrative example; Source: Hassanieh <i>et al.</i> (2017) | 10 |
| 6.1 | Probability distribution v/s angle of arrival: Setting 1, Simulation 1 | 14 |
| 6.2 | Probability distributions corresponding to each hashing: Setting 1, Simulation 1 | 15 |
| 6.3 | Probability distribution v/s angle of arrival: Setting 2, Simulation 1 | 15 |
| 6.4 | Probability distribution v/s angle of arrival: Setting 3, Simulation 1 | 16 |
| 6.5 | Probability distribution v/s angle of arrival: Setting 3, Simulation 2 | 16 |
| 6.6 | Probability distribution v/s angle of arrival: Setting 4, Simulation 1 | 17 |
| 6.7 | Probability distribution v/s angle of arrival: Setting 4, Simulation 2 | 17 |
| 6.8 | Probability distribution v/s angle of arrival: Setting 4, Simulation 3 | 18 |
| 6.9 | Probability distribution v/s angle of arrival: Setting 4, Simulation 4 | 18 |
| 6.10 | Probability distribution v/s angle of arrival: Setting 4, Simulation 5 | 19 |
| 6.11 | Probability distribution v/s angle of arrival: Setting 5, Simulation 1 | 19 |
| 6.12 | Probability distribution v/s angle of arrival: Setting 5, Simulation 2 | 20 |

ABBREVIATIONS

| | |
|---------------|--------------------------------|
| 5G | 5th Generation |
| MHz | Mega Hertz |
| GHz | Giga Hertz |
| Tx | Transmitter |
| Rx | Receiver |
| mmWave | Millimeter Wave |
| MIMO | Multiple Input Multiple Output |
| CFO | Carrier Frequency Offset |
| SNR | Signal to Noise Ratio |
| LoS | Line of Sight |

NOTATION

Bold face lower case letters

Bold face upper case letters

λ

N

K

B

d

α

θ

a

Vectors

Matrices

Wavelength, m

Number of Rx antennas

Total Number of paths between Tx and Rx

Number of bins used to hash the space

spacing between antenna elements in phased array Rx antenna

attenuation factor of the signal

Angle of arrival of the signal

Phase shifter array

CHAPTER 1

INTRODUCTION

1.1 Motivation

The existing wireless networks are nearing saturation with the rapidly increasing demand for bandwidth. This has created a demand for more room. Since the conventional spectrum (i.e. < 3000 MHz) is limited and expensive, high frequency unlicensed spectrum will be used for the next generation (5G and later) cellular networks. The higher frequency spectrum corresponds to the wavelength of the order of millimeters, thus called millimeter wave frequency.

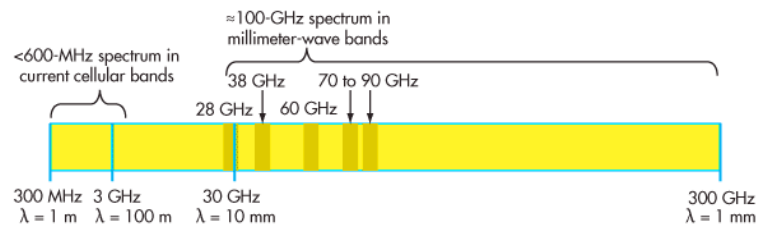


Figure 1.1: EM Spectrum showing vast availability of mmWaves. Source: Electronic Design 'What to Expect with 5G'

Since the millimeter waves exist in higher frequencies, they attenuate very quickly. To achieve significant gain at the transmitter for viable communication, the transmitter must focus their power towards the receiver using highly directional pencil beams. Due to the use of narrow beams, communication is possible only when the transmitter's and receiver's beams are well-aligned. Prevailing radios have to scan the space to find the best alignment between the transmitter's and receiver's beams, a process which takes up to a few seconds. A delay of seconds is undesirable and unacceptable in a system where the number of users is very high and mobile, and the latency required is minimal.

We simulate a beam-steering algorithm, Agile Link, discussed in the paper by Abari *et al.* (2016).

1.2 Beam Formation and Steering

Initial mmWave radios used horn antennas for beam forming, which required mechanical steering. This was a slow and a tedious task. Today, radios use phased array antennas for beam forming which can be steered electronically and is quick. Even with these electronically steered systems, it takes upto a few seconds to scan the space to find the best beam alignment, if conventional beam steering algorithms are used. Agile-Link algorithm reduces this time by multiple orders.

In a mmWave system, the size of an antenna is very small. Thus, a small phased array antenna device of the size of a credit card, can have upto hundreds of antennas. Beam steering for electronic phased array antennas is done using phase shifters, which adds a controllable phase to each antenna. To achieve the condition of best beam alignment, these phase shifters must be set to the correct phase setting, as will be discussed later. **The best beam alignment maximizes the power.**

1.3 Thesis Outline

This thesis has been organized as follows:

- Chapter 2 - System: This chapter mentions about the system details and the assumptions used in the simulation. This system is used for verification of the Agile-Link algorithm.
- Chapter 3 - Agile-Link Algorithm: This chapter discusses the Agile-Link algorithm in detail.
- Chapter 4 - Literature Survey: This chapter enumerates the sources from which the concepts required for this thesis were taken.
- Chapter 5 - Experiments: This chapter contains the details of the system parameters used for different iterations of simulations.
- Chapter 6 - Simulation Results: This chapter showcases the graphs and results obtained on performing the simulations using the system parameters mentioned in the previous chapter.
- Chapter 7 - Conclusion: This chapter mentions the conclusions based on the simulation results.

CHAPTER 2

SYSTEM

The system is made up of a transmitter (Tx) and a receiver (Rx). The Tx simulated is omnidirectional, which transmits in all directions. The Rx simulated is a phased array antenna with N antenna elements.

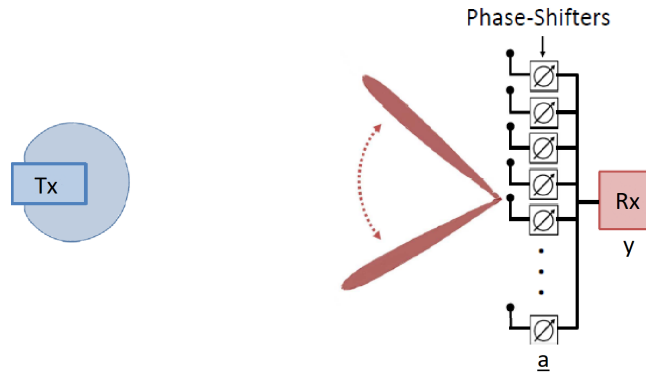


Figure 2.1: Omnidirectional Tx and Phased Array Rx Antenna

The wireless channel at millimeter wave frequencies follows a geometric model according to Alkhateeb *et al.* (2014) Thus, the channel at the receiver antenna array can be modeled as:

$$h_n = \sum_k^K \alpha_k e^{j(2\pi \cos(\theta_k)nd/\lambda + \psi_k)} \quad (2.1)$$

where,

n : receiver antenna element in consideration, can vary from 1 to N

N : Total number of antenna elements in the receiver

k : The path between Tx and Rx in consideration, can vary from 1 to K

K : Total number of paths between Tx and Rx

α_k : attenuation of the received signal along the k -th path

ψ_k : phase of the received signal along the k -th path

θ_k : direction of arrival of the received signal with respect to Rx antenna array along the k -th path

λ : wavelength of wave

$d = \lambda/2$: distance between Rx antenna elements

At millimeter wave frequencies the total number of paths, K , is limited to 4. This is suggested by most empirical studies which show that at mmWave frequencies the channel has only 2 to 3 paths. Rangan *et al.* (2014) Anderson and Rappaport (2004) Sur *et al.* (2015) Sur *et al.* (2016) Abari *et al.* (2016)

At receiver, the final output is y , and is given by:

$$y = \mathbf{a}\mathbf{h} \quad (2.2)$$

The output of each antenna element cannot be measured separately. In a phased array, the combined signal can only be measured after the phase shifters.

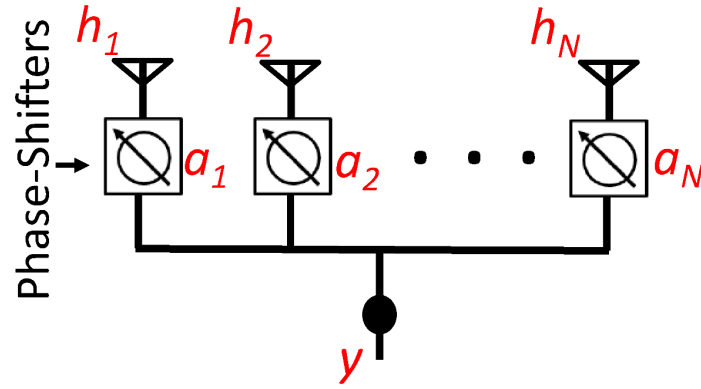


Figure 2.2: Phased Array Architecture; Source: Abari *et al.* (2016)

CHAPTER 3

Agile-Link Algorithm

3.1 The Algorithm

Agile-Link works in two stages:

Stage 1: Randomly hashing the whole space/directions into bins such that each bin collects power from a range/set of directions.

Stage 2: Using voting to recover the directions that have energy, thus finding a suitable direction for communication.

3.1.1 Hashing Spatial Directions into Bins

The space is quantized into directions, and hashed into bins. Each bin corresponds to the energy received in the directions associated with it. An ideal situation while hashing will be to create wide beams that hash the space. The problem is, creating wide beams is difficult since we don't have control over the receiver, except setting the phase of the vector \mathbf{a} (the phase shifter vector). Each setting of this phase shifter vector will create a different beam pattern and the magnitude-squared of the output, i.e. $|y|^2$, corresponds to the energy in the regions covered by the beam pattern.

The different measurements taken over time will accumulate a random unknown phase which will corrupt the phase of the measurements. This is due to CFO (Carrier Frequency Offset) between the transmitter and the receiver, which changes the phase of the received signal. Recovering this phase is a tedious task. So, **the algorithm uses only the magnitude of these measurements**. Abari *et al.* (2016)

In this step, the vector \mathbf{a} (phase shifter vector) must be set such that:

1. good beam patterns are created that can hash the space and cover all regions in space
2. the beam patterns can be randomized to change the different directions that hash to the same bins

In theory, the vector \mathbf{a} must be set such as to create a wider beam to hash many directions into a single bin as shown in figure 3.1. This will require modifying the array size, which is not feasible in the system, as mentioned before. Rather, the algorithm in the paper suggests division of the antenna array into R sub-arrays and direct each sub-array beam toward a different direction. Let the vector \mathbf{a} be divided into R sub-arrays, each of length N/R i.e., $a[1 : N/R]$, $a[N/R + 1 : 2N/R]$, \dots , $a[(R - 1)N/R : N]$. Each segment then sets its beam towards a different direction.

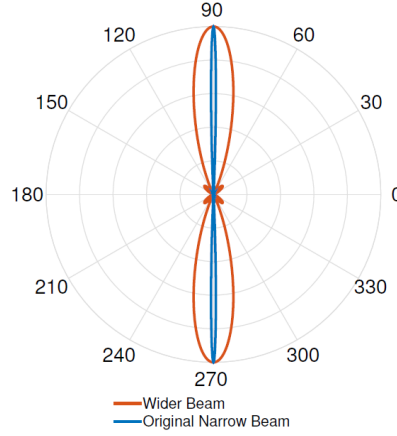


Figure 3.1: A wider beam to hash the space cannot be created since it requires changing the size of the array; Source: Abari *et al.* (2016)

The size of the phase shifter vector is $1 \times N$. Each element of this vector is of the form $\mathbf{a}_n = e^{j\phi_n}$ as mentioned by: Abari *et al.* (2016), Rajagopal (2012). Each element of \mathbf{a} generates a beam in the direction, say θ and $(2\pi - \theta)$. The exact entry in each element of \mathbf{a} is as follows:

$$a_n = e^{j \cdot (n-1) \cdot (d/\lambda) \cdot \pi \cdot \cos(\theta)} \quad (3.1)$$

In the above equation, 3.1, θ is the direction in which a beam is generated. 3.1 has been taken from Rajagopal (2012).

Note that, when the beams created by the sub-arrays are directed in nearby or consecutive directions, it creates bad beams. This is because there is interference of side-lobes due to a sub-array beam with the main-lobe of a neighbouring sub-array beam. So, the algorithm suggests that the sub-arrays direct their beams in well-spaced directions, preferably 60° apart as shown in figure 3.2.

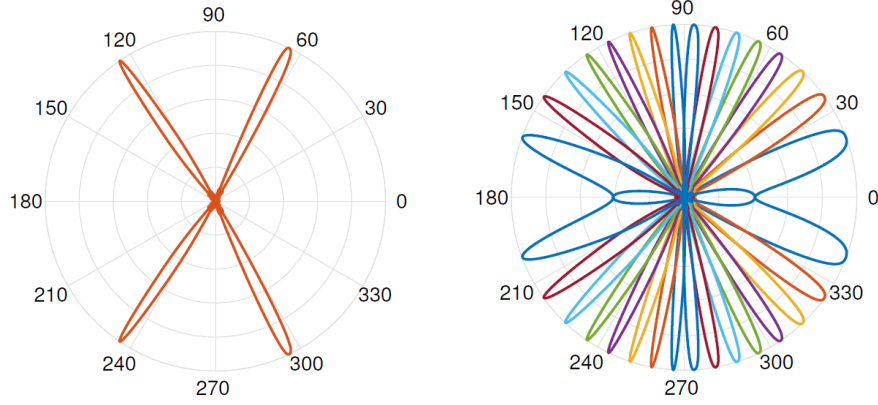


Figure 3.2: 'Hashing well-spread functions into a bin. The beams in the first figure are 60° apart' and 'Bins in a hash function. The beams with the same colour are hashed into the same bin'; Source: Abari *et al.* (2016)

Now, why does the algorithm randomize the bins? There might be a case when multiple destructively interfering paths may be present in the same bin and cancel out each other, showing negligible energy in the bin. If the hashing is not randomized, the colliding paths may remain hidden in all the hashing and an important direction may not be retrieved. With randomized hashing, two colliding paths will not continue to cancel out each other in all the hashing, and in some hashing will be in different bins, thus indicating of its presence.

How does the algorithm randomize the beams that hash directions into bins? The vector \mathbf{a} is a function of 'phase'. This phase of an antenna element corresponds to the beam direction it points to. Randomizing the beams hashing directions, is similar to performing permutation of vector \mathbf{a} . This permutation can be easily done on the phase vector, say ϕ , which has one-to-one relation with vector \mathbf{a} . If n is the n -th phase shifter, the randomizing/permutation operation, as mentioned in the paper: Abari *et al.* (2016) can be shown as follows:

$$\phi'(n) = \phi(\sigma n \bmod N) - 2\pi\beta n/N \quad (3.2)$$

In the above equation 3.2,

σ : a random number, modulo N

β : a random number, $< N$

Using the above method, we can generate L different random permutations of the

vector \mathbf{a} . This is based on the L different possible values of σ . The maximum value of L is the maximum possible values of σ .

3.1.2 Recovering the Directions of the Paths

After hashing the spatial directions into bins, the algorithm finds the actual directions of the signal using a voting based scheme, where each bin votes for the directions hashed into it. After L random hashes, the directions that have the highest votes will be the directions of arrival of the signal.

However, there is an issue with such method of 'hard-voting'. The side-lobes of the beams create leakage between the bins and a strong path in one bin can leak energy into other bins corrupting the voting process. To take the leakage into consideration, the algorithm uses 'soft-voting' as mentioned below.

The algorithm, Agile-Link, models the beam patterns as a probability distribution $P(\theta)$. $P(\theta)$ is the measure of probability that the arrival direction of the received signal is θ . When the signal is hashed into B bins, B such (randomized) patterns collect B different measurements, $y_{1 \times B}$, corresponding to the bins. We can compute the probability of the signal coming from angle θ by calculating the magnitude squared of each measurement and normalizing their power. This can be done as follows:

$$Pr(\theta) = \frac{1}{\|y\|_2^2} \sum_{b=1}^B |y_b|^2 \times P_b(\theta) \quad (3.3)$$

In equation 3.3,

$P_b(\theta)$ is the beam pattern (probability distribution) corresponding to b -th bin,

$\|y\|_2^2$: L2-norm-squared of y .

The summation is taken over the individual bin-probabilities, since the direction of the signal can fall into any of the bins.

After performing a few random hashes (say, L random hashes), the final probability distribution of the signal direction can be computed as follows:

$$Pr(\theta) = \prod_{l=1}^L \frac{1}{\|y_l\|_2^2} \sum_{b=1}^{B_l} |y_{b,l}|^2 \times P_{b,l}(\theta) \quad (3.4)$$

In equation 3.4,

L: Total number of hashes performed by the algorithm,

The product is taken over the probabilities of each hashing, so that inputs from all the hashing is taken into account. Also, each hashing might have some false-positive results (direction), which will be nullified when multiple hashing is done.

Finally, the K directions of θ that have the highest probabilities will correspond to the directions of the K paths that the signal traverses and is incident on the receiver. The best beam alignment is then chosen to be the direction of the path that delivers the maximum energy out of these K different directions.

3.2 Illustrative Example

To understand the Agile-Link's algorithm, an example can be as follows:

Consider a receiver antenna array with $N = 16$ antenna elements, The received signal has a dominant path along the direction of 60° . The algorithm has to find that the signal has arrived via this 60° direction path. This finding will be used to steer the beam in this direction, to achieve the best SNR and establish a connection.

Firstly, the spatial directions must be hashed into bins, and each bin will then collect energy from these hashed directions. For example, if the space is hashed into 4 bins, then each bin would collect energy from $N/4 = 4$ different directions. This can be done by setting the phase shifter vector to steer the receiver antenna in 4 different directions.

Now, a bin will contain energy only if the signal's path matches a direction that is hashed to the bin. The directions that hash into a bin, will be changed every time during the randomized hashing. If a direction truly contains energy due to the presence of the signal, the bin in which it is present will get votes during voting. After analyzing the voting results, it is possible to figure out the common directions in all the highly-voted bins. These common directions will give the dominant paths of the signal.

Figure 3.3 illustrates the working of the algorithm.

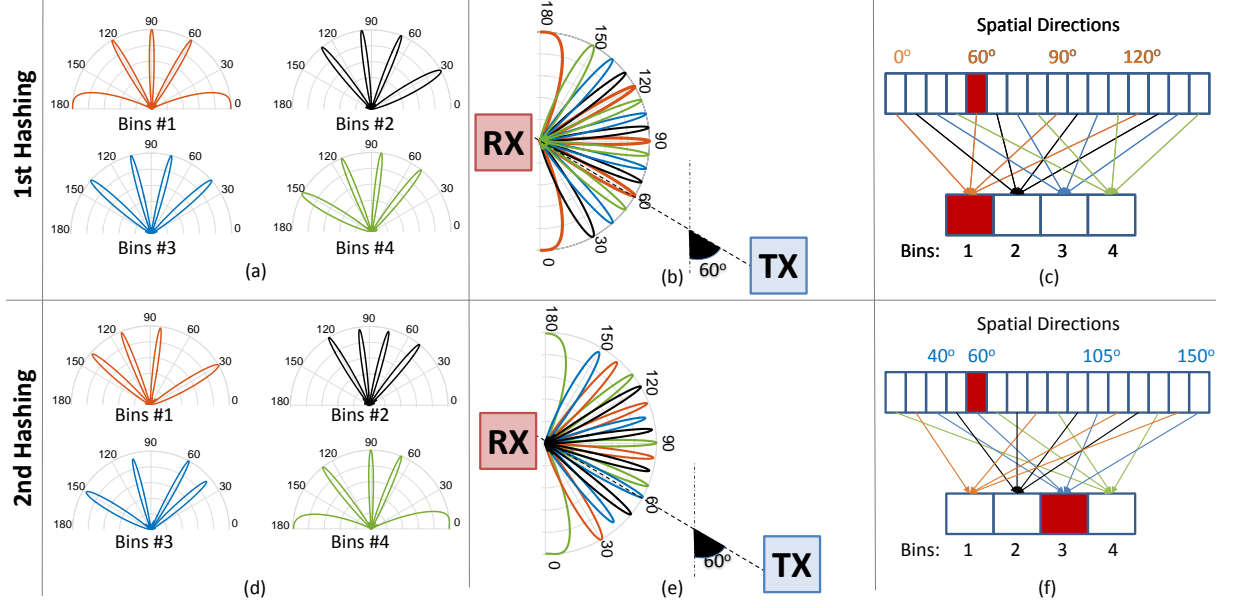


Figure 3.3: Illustrative example; Source: Hassanieh *et al.* (2017)

3.3 Measurement Complexity

According to the paper, Abari *et al.* (2016):

Agile-Link's algorithm takes B measurements for each hashing of the space, where B is the number of bins. In the case where both Tx and Rx have antenna arrays, Agile-Link takes $B \times B$ measurements. The hashing is repeated L times, for a total number of measurements $L \times B^2$. Since the channel is sparse with only K paths, setting $B = O(K)$ is done to ensure a small number of path collisions in the same bin. Also, $L = \log N$ is set to ensure that the probability of missing a path is polynomially small. Thus, Agile-Link's algorithm requires $O(K^2 \log N)$ measurements, which scales sub-linearly with the size of the array. Hence, for large N , it delivers significant gains compared to the exhaustive search, or the 802.11ad standard.

CHAPTER 4

LITERATURE SURVEY

Basic communication systems ideas were taken from Madhow (2014), Proakis and Salehi (2002).

5G, wireless and cellular communication related concepts were taken from Rappaport (2010), Goldsmith (2005), Molisch (2005), Tse and Viswanath (2005).

Agile Link algorithm is introduced in Abari *et al.* (2016). A similar version also appears in Hassanieh *et al.* (2017).

Beamforming and setting up of phase shifter array (vector \mathbf{a}) is taken from Rajagopal (2012).

The channel model for a millimeter wave is discussed in Alkhateeb *et al.* (2014). Also, the number of dominant paths in channel for a millimeter wave is discussed in Rangan *et al.* (2014), Anderson and Rappaport (2004), Sur *et al.* (2015), Sur *et al.* (2016).

CHAPTER 5

EXPERIMENTS

The following data is considered for the simulation. The results mentioned in this thesis are from simulations using these values:

Common Settings :

$$d/\lambda = 0.5$$

$$N = 16$$

$$\sigma = [3, 5, 7, 9, 11, 13, 15] \quad (\text{Possible values of } \sigma)$$

1. Setting 1, Simulation 1:

$$K = 2$$

$$\alpha = [0.1, 2]$$

$$\theta = [20^\circ, 50^\circ]$$

$$B = 8 \quad (\text{Number of bins})$$

$$L = 7 \quad (\text{Number of times hashing done})$$

2. Setting 2, Simulation 1:

$$K = 2$$

$$\alpha = [0.1, 2]$$

$$\theta = [40^\circ, 100^\circ]$$

$$B = 8 \quad (\text{Number of bins})$$

$$L = 7 \quad (\text{Number of times hashing done})$$

3. Setting 3, Simulations 1,2:

$$K = 2$$

$$\alpha = [1, 2]$$

$$\theta = [40^\circ, 120^\circ]$$

$$B = 8 \quad (\text{Number of bins})$$

$$L = 7 \quad (\text{Number of times hashing done})$$

4. Setting 4:

$$K = 3$$

$$\alpha = [0.1, 1, 2]$$

$$\theta = [40^\circ, 100^\circ, 140^\circ]$$

(a) Simulation 1,2,3:

$$B = 8 \quad (\text{Number of bins})$$

$$L = 7 \quad (\text{Number of times hashing done})$$

(b) Simulations 3,4:

$$B = 8 \quad (\text{Number of bins})$$

$$L = 4 \quad (\text{Number of times hashing done})$$

(c) Simulation 5:

$$B = 4 \quad (\text{Number of bins})$$

$$L = 4 \quad (\text{Number of times hashing done})$$

5. Setting 5, Simulations 1,2:

$$K = 3$$

$$\alpha = [1, 2, 4]$$

$$\theta = [40^\circ, 100^\circ, 140^\circ]$$

$$B = 8 \quad (\text{Number of bins})$$

$$L = 7 \quad (\text{Number of times hashing done})$$

CHAPTER 6

SIMULATION RESULTS

According to the system parameters in the previous chapter, the simulation results are shown as follows:

1. Setting 1, Simulation 1: $K = 2$, $\alpha = [0.1, 2]$, $\theta = [20^\circ, 50^\circ]$, $B = 8$, $L = 7$

Fig 6.1 is a plot for the case when the total number of paths considered is 2, i.e. $(20^\circ, 50^\circ)$, and the highly dominant one among them is at 50° . The number of bins used in the algorithm is 8, each consisting of 2 directions each. We do 7 random hashing to find the dominant direction.

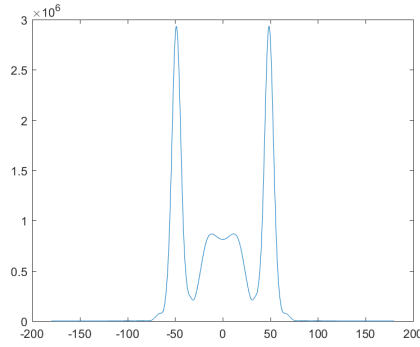


Figure 6.1: Probability distribution v/s angle of arrival: Setting 1, Simulation 1

The observation is as **expected** and **satisfactory** from the plot in Fig 6.1: Strong peaks at $[40^\circ, -40^\circ]$, and small peaks at $[20^\circ, -20^\circ]$.

Each plot is symmetric about the centre of the x-axis. This shows that beam generation is done at θ and $(2\pi - \theta)$, and is decoded together.

Plots in Fig 6.2 are outputs at the end of each hashing. Some 'individual hashing' plots give incorrect output directions, because of the leakage problem, as mentioned in subsection 3.1.2. This problem is solved with multiple hashing.

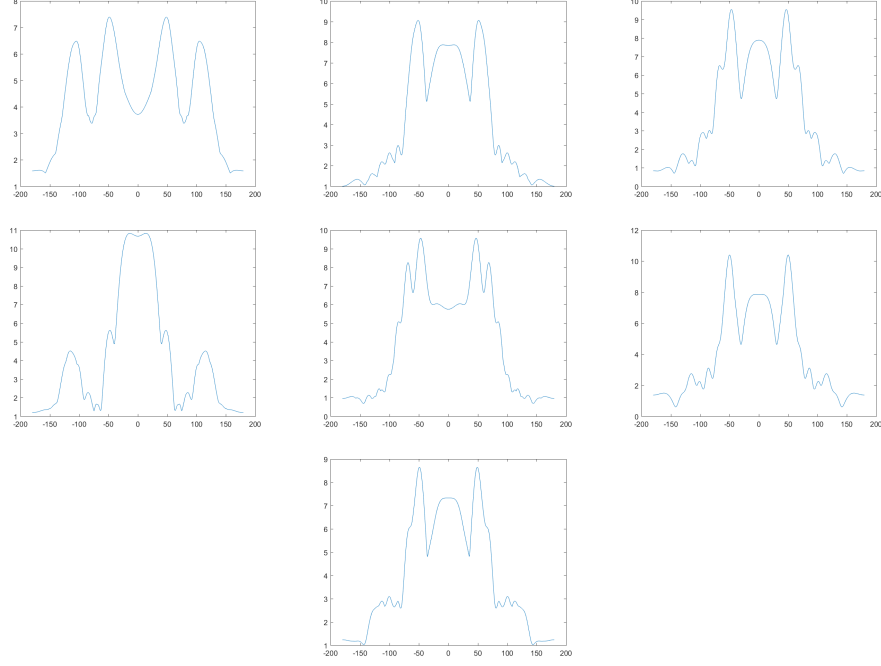


Figure 6.2: Probability distributions corresponding to each hashing: Setting 1, Simulation 1

2. Setting 2, Simulation 1: $K = 2$, $\alpha = [0.1, 2]$, $\theta = [40^\circ, 100^\circ]$, $B = 8$, $L = 7$

Fig 6.3 is a plot for the case when the total number of paths considered is 2, i.e. $(40^\circ, 100^\circ)$, and the highly dominant one among them is at 100° . The number of bins used in the algorithm is 8, each consisting of 2 directions each. We do 7 random hashing to find the dominant direction.

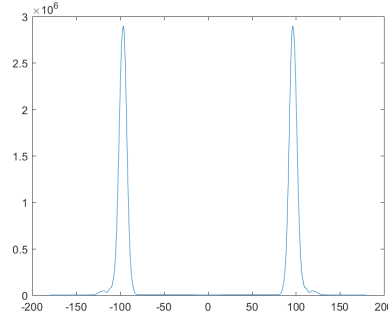


Figure 6.3: Probability distribution v/s angle of arrival: Setting 2, Simulation 1

The observation is as expected and **satisfactory** from the plot in Fig 6.3: Strong peaks at $[100^\circ, -100^\circ]$, and negligibly small peaks at $[40^\circ, -40^\circ]$.

From Figs 6.1 and 6.3, we can conclude that Agile-Link works well for a mmWave system with LoS communication.

3. Setting 3, Simulation 1: $K = 2$, $\alpha = [1, 2]$, $\theta = [40^\circ, 120^\circ]$, $B = 8$, $L = 7$

Fig 6.4 is a plot for the case when the total number of paths considered is 2, i.e. $(40^\circ, 120^\circ)$. In this case, the energy of the signal along both paths is of the same order of magnitude. The number of bins used in the algorithm is 8, each consisting of 2 directions each. We do 7 random hashing to find the dominant direction.

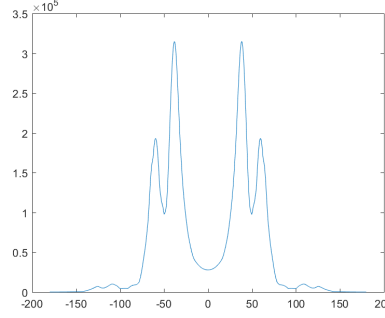


Figure 6.4: Probability distribution v/s angle of arrival: Setting 3, Simulation 1

The observation is not as expected and **unsatisfactory** from the plot in Fig 6.4: Strong peaks were expected at $[120^\circ, -120^\circ]$, and relatively smaller peaks at $[40^\circ, -40^\circ]$, but the former peaks are completely missing.

4. Setting 3, Simulation 2: $K = 2$, $\alpha = [1, 2]$, $\theta = [40^\circ, 120^\circ]$, $B = 8$, $L = 7$

Fig 6.5 is a plot for the case with similar settings as the previous one.

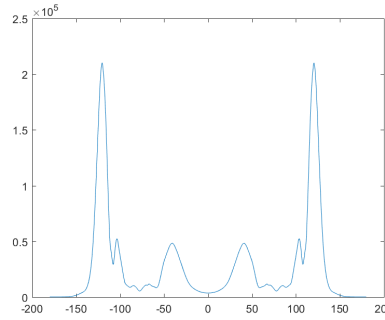


Figure 6.5: Probability distribution v/s angle of arrival: Setting 3, Simulation 2

The observation is as expected and **satisfactory** from the plot in Fig 6.5: Strong peaks are seen at $[120^\circ, -120^\circ]$, and relatively smaller peaks at $[40^\circ, -40^\circ]$.

From the two Figs 6.4 and 6.5, we can conclude that as the number of effective paths increased from Setting 1 to 2, the algorithm's accuracy reduced.

5. Setting 4, Simulation 1: $K = 3$, $\alpha = [0.1, 1, 2]$, $\theta = [40^\circ, 100^\circ, 140^\circ]$, $B = 8$, $L = 7$

Fig 6.6 is a plot for the case when the total number of paths considered is 3, i.e. $(40^\circ, 100^\circ, 140^\circ)$. In this case, the energy of the signal along the paths $(100^\circ, 140^\circ)$ is of the same order of magnitude, and along (40°) is significantly smaller. The number of bins used in the algorithm is 8, each consisting of 2 directions each. We do 7 random hashing to find the dominant direction.

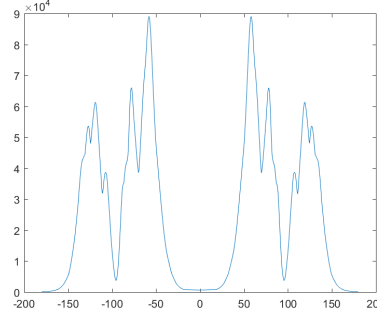


Figure 6.6: Probability distribution v/s angle of arrival: Setting 4, Simulation 1

The observation is not as expected and **unsatisfactory** from the plot in Fig 6.4: Strong visible peaks were expected at $[140^\circ, -140^\circ]$, and at $[100^\circ, -100^\circ]$, with peaks at the latter angle shorter than the former.

6. Setting 4, Simulation 2: $K = 3$, $\alpha = [0.1, 1, 2]$, $\theta = [40^\circ, 100^\circ, 140^\circ]$, $B = 8$, $L = 7$

Fig 6.7 is a plot for the case with similar settings as the previous one.

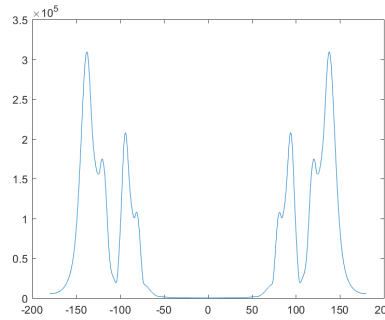


Figure 6.7: Probability distribution v/s angle of arrival: Setting 4, Simulation 2

The observation is as expected and **satisfactory** from the plot in Fig 6.7: Strong peaks are seen at $[140^\circ, -140^\circ]$, relatively smaller peaks at $[100^\circ, -100^\circ]$.

7. Setting 4, Simulation 3: $K = 3$, $\alpha = [0.1, 1, 2]$, $\theta = [40^\circ, 100^\circ, 140^\circ]$, $B = 8$, $L = 4$

Fig 6.8, is a plot for the case when the total number of paths considered is 3, i.e. $(40^\circ, 100^\circ, 140^\circ)$. In this case, the energy of the signal along the paths $(100^\circ, 140^\circ)$ is of the same order of magnitude, and along (40°) is significantly smaller. The number of bins used in the algorithm is 8, each consisting of 2 directions each. We do **only 4 random hashing (instead of 7)** to find the dominant direction.

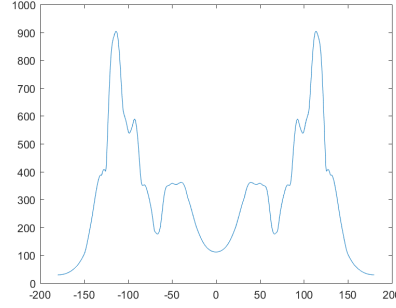


Figure 6.8: Probability distribution v/s angle of arrival: Setting 4, Simulation 3

The output from this simulation is **sub-optimal**. The leakage problem (Subsection 3.1.2, can be seen here: the directions around the desired ones, also have significant probabilities.

8. Setting 4, Simulation 4: $K = 3$, $\alpha = [0.1, 1, 2]$, $\theta = [40^\circ, 100^\circ, 140^\circ]$, $B = 8$, $L = 4$

Fig 6.9 is a plot for the case with similar settings as the previous one.

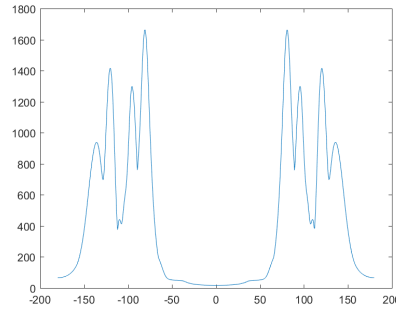


Figure 6.9: Probability distribution v/s angle of arrival: Setting 4, Simulation 4

The output from this simulation is **unsatisfactory**. The leakage problem (Subsection 3.1.2 along with errors due to more number of paths can be seen here. The expected plot must look like: Fig 6.7.

9. Setting 4, Simulation 5: $K = 3$, $\alpha = [0.1, 1, 2]$, $\theta = [40^\circ, 100^\circ, 140^\circ]$, $B = 4$, $L = 4$

Fig 6.10 is a plot for the case with similar settings as the previous one, except the number of bins. The number of bins in this case is 4, with 4 directions each.

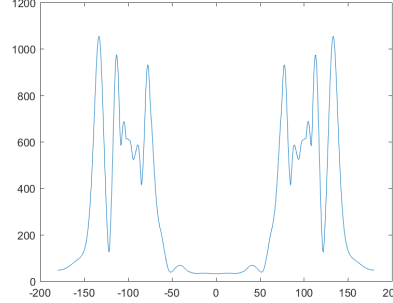


Figure 6.10: Probability distribution v/s angle of arrival: Setting 4, Simulation 5

The output in this case is **unsatisfactory**. The leakage problem has intensified, along with errors due to more number of paths.

10. Setting 5, Simulation 1: $K = 3$, $\alpha = [1, 2, 4]$, $\theta = [40^\circ, 100^\circ, 140^\circ]$, $B = 8$, $L = 7$

Fig 6.11, is a plot for the case when the total number of paths considered is 3, i.e. ($40^\circ, 100^\circ, 140^\circ$). In this case, the energy of the signal along all the paths is of the same order of magnitude. The number of bins used in the algorithm is 8, each consisting of 2 directions each. We do 7 hashing to find the dominant direction.

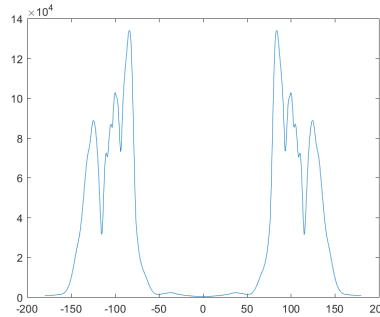


Figure 6.11: Probability distribution v/s angle of arrival: Setting 5, Simulation 1

The result of this experiment is **unsatisfactory**. This is due to increased effective number of paths from 2 to 3.

11. Setting 5, Simulation 2: $K = 3$, $\alpha = [1, 2, 4]$, $\theta = [40^\circ, 100^\circ, 140^\circ]$, $B = 8$, $L = 7$

Fig 6.12 is a plot for the case with similar settings as the previous one.

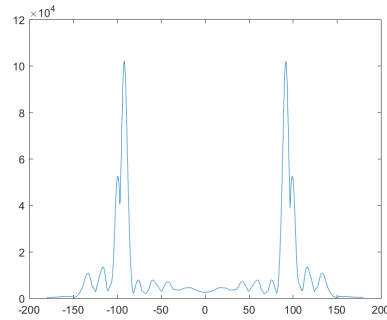


Figure 6.12: Probability distribution v/s angle of arrival: Setting 5, Simulation 2

The result of this experiment is **unsatisfactory**.

From Figs 6.11 and 6.12, we can conclude that as the number of paths reach 3, the accuracy of the algorithm reduces drastically.

The acceptable results are achieved in the following trials:

- Simulation 1
- Simulation 2
- Simulation 3, Experiment 2
- Simulation 4, Experiment 2
- Simulation 4, Experiment 3

CHAPTER 7

CONCLUSION

We demonstrate that the Agile-Link algorithm works well with smaller values of K i.e. situation with fewer total paths. This also shows that the Agile-Link algorithm works well with LoS situation, and is able to identify LoS signal direction accurately. As the value of K increases, there are some simulations which do not give expected output. Also, as the number of hashing increases, the output direction is more accurate.

REFERENCES

1. **Abari, O., H. Hassanieh, M. Rodeguez, and D. Katabi** (2016). Millimeter wave communications: From point-to-point links to agile network connections. *Proceedings of the 15th ACM Workshop on Hot Topics in Networks*.
2. **Alkhateeb, A., O. E. Ayach, G. Leus, and R. W. Heath** (2014). Channel estimation and hybrid precoding for millimeter wave cellular systems. *Selected Topics in Signal Processing, IEEE Journal of 2014*.
3. **Anderson, C. R. and T. S. Rappaport** (2004). In-building wideband partition loss measurements at 2.5 and 60 ghz. *IEEE Transactions on Wireless Communications Volume 3 Issue 3*.
4. **Goldsmith, A.**, *Wireless Communications*. Cambridge University Press, 2005.
5. *Electronic Design 'What to Expect with 5G'* (retrieved: 2018-05-08). URL <http://www.electronicdesign.com/communications/what-expect-5g>.
6. **Hassanieh, H., O. Abari, M. Rodreguez, M. Abdelghany, D. Katabi, and P. Indyk** (2017). Agile millimeter wave networks with provable guarantees.
7. **Madhow, U.**, *Introduction to Communication Systems*. Cambridge University Press, 2014.
8. **Molisch, A.**, *Wireless Communications*. Wiley, 2005.
9. **Proakis, J. G. and M. Salehi**, *Communication Systems Engineering, 2nd Edition*. Prentice Hall, 2002.
10. **Rajagopal, S.** (2012). Beam broadening for phased antenna arrays using multi-beam subarrays. *In ICC 2012*.
11. **Rangan, S., T. S. Rappaport, and E. Erkip** (2014). Millimeter-wave cellular wireless networks: Potentials and challenges. *Proceedings of the IEEE Volume 102 Issue 3*, 366–385.
12. **Rappaport, T.**, *Wireless Communications - Principles and Practice (2nd Edition)*. Pearson, 2010.
13. **Sur, S., V. Venkateswaran, X. Zhang, and P. Ramanathan** (2015). 60 ghz indoor networking through flexible beams: A link-level profiling. *In Sigmetrics: Proceedings of the 2015 ACM SIGMETRICS International Conference on Measurement and Modeling of Computer Systems*.
14. **Sur, S., X. Zhang, P. Ramanathan, and R. Chandra** (2016). Beamspy: enabling robust 60 ghz links under blockage. *In NSDI: Proceedings of the 13th Usenix Conference on Networked Systems Design and Implementation*.
15. **Tse, D. and P. Viswanath**, *Fundamentals of Wireless Communications*. Cambridge University Press, 2005.